

¹ MotilA – A Python pipeline for the analysis of
² microglial fine process motility in 3D time-lapse
³ multiphoton microscopy data

⁴ Fabrizio Musacchio  ¹, Sophie Crux¹, Felix Nebeling¹, Nala Gockel¹, Falko
⁵ Fuhrmann¹, and Martin Fuhrmann  ¹

⁶ 1 German Center for Neurodegenerative Diseases (DZNE), Bonn, Germany ¶ Corresponding author

DOI: [10.xxxxxx/draft](https://doi.org/10.xxxxxx/draft)

Software

- [Review](#) 
- [Repository](#) 
- [Archive](#) 

Editor: [Open Journals](#) 

Reviewers:

- [@openjournals](#)

Submitted: 01 January 1970

Published: unpublished

License

Authors of papers retain copyright
and release the work under a
Creative Commons Attribution 4.0
International License ([CC BY 4.0](#)).
18
19
20
21

⁷ Summary

⁸ *MotilA* is an open-source Python pipeline for quantifying microglial fine-process motility in
⁹ 4D (TZYX) or 5D (TZCYX) time-lapse fluorescence microscopy data, supporting both single-
¹⁰ channel and two-channel acquisition. It was developed for high-resolution *in vivo* multiphoton
¹¹ imaging and supports both single-stack and cohort-scale batch analyses. The workflow
¹² performs sub-volume extraction, optional registration and spectral unmixing, a maximum-
¹³ intensity projection along the Z-axis, segmentation, and pixel-wise change detection to compute
¹⁴ the turnover rate (TOR). *MotilA* specifically targets pixel-level process motility rather than
¹⁵ object tracking or full morphometry. The code is platform independent, documented with
¹⁶ tutorials and example datasets, and released under GPL-3.0.

¹⁷ Statement of need

¹⁸ Microglia are immune cells of the central nervous system and continuously remodel their
processes to survey brain tissue and respond to pathology ([M. Fuhrmann et al., 2010](#); [Nimmer-
jahn et al., 2005](#); [Prinz et al., 2019](#); [Tremblay et al., 2010](#)). Quantifying this subcellular motility
is important for studies of neuroinflammation, neurodegeneration, and synaptic plasticity. Cur-
rent practice in many labs relies on manual or semi-manual measurements in general-purpose
tools such as Fiji/ImageJ or proprietary software ([Carl Zeiss Microscopy GmbH, Accessed
2025](#); [Schindelin et al., 2012](#)). These procedures are time consuming, hard to reproduce, focus
on single cells, and are sensitive to user bias ([Brown, 2017](#); [Wall et al., 2018](#)). There is no
dedicated, open, and batch-capable solution tailored to this task.

¹⁹ *MotilA* fills this gap with an end-to-end, reproducible pipeline for 3D time-lapse two-channel
imaging. It standardizes preprocessing, segmentation, and motility quantification and scales
from individual stacks to large experimental cohorts. Unlike Fiji/ImageJ macros or proprietary
packages, *MotilA* provides a fully automated non-interactive workflow in Python that applies
identical parameters across datasets, logs all intermediate steps, and avoids user-dependent
adjustments. This ensures reproducible, bias-minimized, and scalable processing of large 3D
time-lapse datasets, including optional motion correction and spectral unmixing. Although
optimized for microglia, the approach generalizes to other motile structures that can be reliably
segmented across time.
20
21
22
23
24
25
26
27
28
29
30
31
32
33
34
35

³⁶ To clarify *MotilA*'s novelty relative to existing analysis approaches, the following table summa-
³⁷ rizes key differences between *MotilA*, Fiji/ImageJ, and ZEISS ZEN:

³⁸ **Table 1.** Comparison of MotilA with commonly used alternatives for microglial motility analysis.

Feature	Fiji/ImageJ	ZEISS ZEN	MotilA
Automation	Limited. User-recorded macros; complex workflows often require manual steps and must be split across several macros.	None. Full user interaction required.	Full. End-to-end non-interactive workflow.
Batch processing	Limited. Macros can process several files in one folder, but they cannot navigate nested directory structures or manage multi-step 3D multi-channel time-series pipelines.	None. Each dataset processed manually.	Full. Metadata-driven cohort processing.
Reproducibility	Moderate. Requires complete manual logging; interactive tuning reduces reproducibility.	Low. Manual adjustments introduce strong user bias.	High. Full parameter logging and deterministic runs.
Scalability	Low. Full-stack RAM loading; no chunked I/O for large 3D data.	Low-medium. Efficient viewing but no automated processing for large time-lapse datasets.	High. Chunked I/O for multi-gigabyte 3D two-channel stacks.
Open-source	Yes (GPL-3.0).	No (proprietary).	Yes (GPL-3.0).

³⁹ Implementation and core method

⁴⁰ Input is a 5D stack in TZCYX or a 4D stack in TZYX order, where T is time, Z is depth, C is channel, and YX are spatial dimensions. *MotilA* does not assume a fixed channel order. Users ⁴¹ specify which channel contains microglia and which, if present, provides a structural reference ⁴² signal, such as a neuronal label. Although the reference channel does not enter the motility ⁴³ computation, it is commonly acquired in microglial imaging because it offers stable features ⁴⁴ that support robust pre-processing registration of the 3D stack before it is passed to *MotilA*. ⁴⁵ The additional channel may also be used for optional spectral unmixing in the presence of ⁴⁶ bleed-through.

⁴⁷ For each time point, *MotilA* extracts a user-defined z-sub-volume, optionally performs 3D ⁴⁸ motion correction and spectral unmixing, and computes a 2D maximum-intensity projection ⁴⁹ along the Z-axis to enable interpretable segmentation. After thresholding, the binarized ⁵⁰ projection $B(t_i)$ is compared with $B(t_{i+1})$ to derive a change map

$$\Delta B(t_i) = 2B(t_i) - B(t_{i+1}).$$

⁵² Pixels are classified as stable “S” ($\Delta B = 1$), gained “G” ($\Delta B = -1$), or lost “L” ($\Delta B = 2$). ⁵³ From these counts, the turnover rate is defined as

$$TOR = \frac{G + L}{S + G + L},$$

⁵⁴ representing the fraction of pixels that changed between consecutive frames. This pixel-based ⁵⁵ strategy follows earlier microglial motility work (M. Fuhrmann et al., 2010; Nebeling et al., ⁵⁶ 2023) while providing a fully automated and batchable implementation with parameter logging ⁵⁷ and diagnostics.

58 The pipeline exposes options for 3D or 2D registration, contrast-limited adaptive histogram
59 equalization, histogram matching across time to mitigate bleaching, and median or Gaussian
60 filtering (Pizer et al., 1987; van der Walt et al., 2014; Virtanen et al., 2020). Results include
61 segmented images, G/L/S/TOR values, brightness and area traces, and spreadsheets for
62 downstream statistics. Memory-efficient reading and chunked processing of large TIFFs are
63 supported via Zarr (Miles et al., 2025).

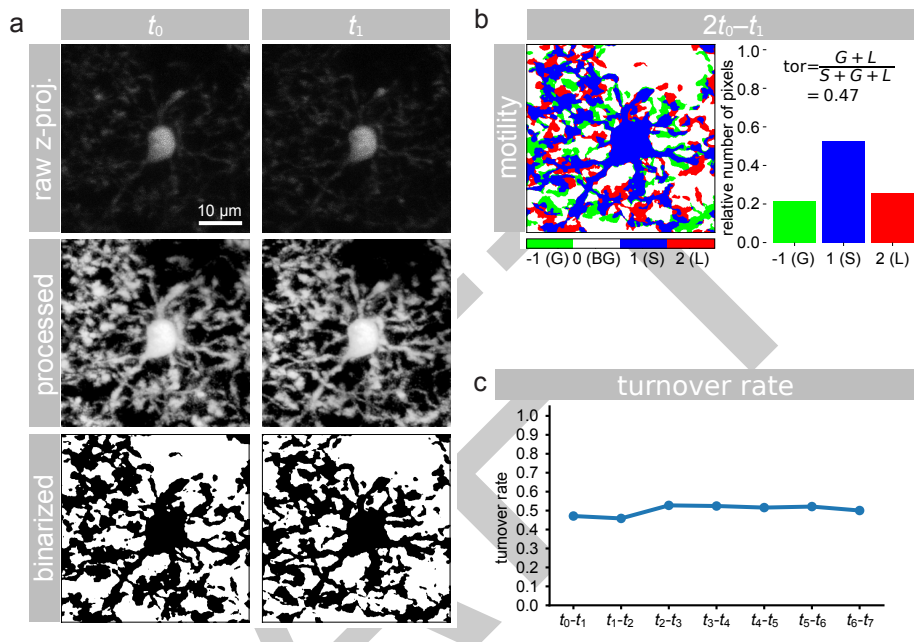


Figure 1: Example analysis with *MotilA*. **a)** z-projected microglial images at two consecutive time points (t_0 , t_1), shown as raw, processed, and binarized data. **b)** pixel-wise classification of gained (G), stable (S), and lost (L) pixels used to compute the turnover rate (TOR). **c)** TOR values across time points from the same dataset, illustrating dynamic remodeling of microglial fine processes.

Usage

64 *MotilA* can be called from Python scripts or Jupyter notebooks. Three entry points cover
65 common scenarios: `process_stack` for a single stack, `batch_process_stacks` for a project
66 folder organized by dataset identifiers with a shared metadata sheet, and `batch_collect` to
67 aggregate metrics across datasets. All steps write intermediate outputs and logs to facilitate
68 validation and reproducibility. *MotilA*'s GitHub repository provides tutorials and an example
69 dataset to shorten onboarding.

Applications and scope

71 *MotilA* has been applied to quantify microglial process dynamics in several *in vivo* imaging
72 studies and preprints (Crux et al., 2024; F. Fuhrmann et al., 2025; Gockel et al., 2025). Typical
73 use cases include baseline surveillance behavior, responses to neuroinflammation or genetic
74 perturbations, and deep three-photon imaging where manual analysis is impractical. The
75 binarize-and-compare principle can in principle be adapted to other structures such as dendrites
76 or axons when segmentation across time is robust.

Limitations

78 *MotilA* quantifies microglial process motility using 2D maximum-intensity projections rather
79 than fully volumetric analysis. This choice reflects practical constraints of two-photon microglial

81 imaging: axial resolution degrades with depth, producing elongated point-spread functions and
82 reduced contrast along Z, which makes reliable voxel-wise 3D segmentation of thin processes
83 difficult. Z-projection increases effective signal per pixel and follows established practice in
84 earlier microglial motility studies (see, e.g., M. Fuhrmann et al. (2010); Nebeling et al. (2023)),
85 but necessarily sacrifices axial specificity and may merge structures that overlap along Z. Users
86 are therefore advised to select sub-volumes with minimal axial overlap.

87 Segmentation quality critically determines the accuracy of motility estimates and can be affected
88 by blood vessels, low signal-to-noise ratios, and intensity drift over time. The current spectral
89 unmixing is implemented as a simple subtraction and may be insufficient for fluorophores with
90 complex spectral overlap. Finally, *MotilA* focuses on pixel-level process motility rather than
91 object-level tracking or full morphological reconstruction. Fully three-dimensional motility
92 analysis would require volumetric segmentation and substantially higher computational resources
93 and is beyond the scope of the current version.

94 Availability

95 Source code, documentation, tutorials, and issue tracking are hosted at: <https://github.com/FabrizioMusacchio/motila>. The software runs on Windows, macOS, and Linux with Python 3.9
96 or newer and standard scientific Python stacks. It is released under GPL-3.0, and contributions
97 via pull requests or issues are welcome. An example dataset used for demonstration and testing
98 purposes is available via Zenodo ([Gockel et al., 2025](#)) and described in the documentation.

100 Acknowledgements

101 We thank the Light Microscopy Facility and Animal Research Facility at the DZNE, Bonn, for
102 essential support. This work was supported by the DZNE and grants to MF from the ERC
103 (MicroSynCom 865618) and the DFG (SFB1089 C01, B06; SPP2395). MF is a member of
104 the DFG Excellence Cluster ImmunoSensation2. Additional support came from the iBehave
105 network and the CANTAR network funded by the Ministry of Culture and Science of North
106 Rhine-Westphalia, and from the Mildred-Scheel School of Oncology Cologne-Bonn. Animal
107 procedures followed institutional and national regulations, with efforts to reduce numbers and
108 refine conditions.

109 References

- 110 Brown, D. L. (2017). Bias in image analysis and its solution: Unbiased stereology. *Journal of Toxicologic Pathology*, 30(3), 183–191. <https://doi.org/10.1293/tox.2017-0013>
- 112 Carl Zeiss Microscopy GmbH. (Accessed 2025). *ZEISS ZEN Microscopy Software*. <https://www.zeiss.com/metrology/en/software/zeiss-zен-core.html>.
- 114 Crux, S., Roggan, M. D., Poll, S., Nebeling, F. C., Schiweck, J., Mittag, M., Musacchio, F.,
115 Steffen, J., Wolff, K. M., Baral, A., Witke, W., Gurniak, C., Bradke, F., & Fuhrmann,
116 M. (2024). Deficiency of actin depolymerizing factors ADF/Cfl1 in microglia decreases
117 motility and impairs memory. *bioRxiv*. <https://doi.org/10.1101/2024.09.27.615114>
- 118 Fuhrmann, F., Nebeling, F. C., Musacchio, F., Mittag, M., Poll, S., Müller, M., Giovannetti, E.
119 A., Maibach, M., Schaffran, B., Burnside, E., Chan, I. C. W., Lagurin, A. S., Reichenbach,
120 N., Kaushalya, S., Fried, H., Linden, S., Petzold, G. C., Tavosanis, G., Bradke, F., &
121 Fuhrmann, M. (2025). Three-photon *in vivo* imaging of neurons and glia in the
122 medial prefrontal cortex with sub-cellular resolution. *Communications Biology*, 8(1), 795.
123 <https://doi.org/10.1038/s42003-025-08079-8>
- 124 Fuhrmann, M., Bittner, T., Jung, C. K. E., Burgold, S., Page, R. M., Mitteregger, G., Haass,
125 C., LaFerla, F. M., Kretzschmar, H., & Herms, J. (2010). Microglial Cx3cr1 knockout
126 prevents neuron loss in a mouse model of Alzheimer's disease. *Nature Neuroscience*, 13(4),
127 411–413. <https://doi.org/10.1038/nn.2511>

- 128 Gockel, N., Nieves-Rivera, N., Druart, M., Jaako, K., Fuhrmann, F., Rožkalne, R., Musacchio,
129 F., Poll, S., Jansone, B., Fuhrmann, M., & Magueresse, C. L. (2025). *Example datasets for*
130 *microglial motility analysis using the MotilA pipeline*. Zenodo. <https://doi.org/10.5281/zenodo.15061566>
- 132 Miles, A., jakirkham, Hamman, J., Orfanos, D. P., Stansby, D., Bussonnier, M., Moore,
133 J., Bennett, D., Augspurger, T., Rzepka, N., Cherian, D., Verma, S., Bourbeau, J.,
134 Fulton, A., Abernathey, R., Lee, G., Spitz, H., Kristensen, M. R. B., Jones, M., &
135 Schut, V. (2025). *Zarr-developers/zarr-python: v3.1.5* (Version v3.1.5). Zenodo. <https://doi.org/10.5281/zenodo.17672242>
- 137 Nebeling, F. C., Poll, S., Justus, L. C., Steffen, J., Keppler, K., Mittag, M., & Fuhrmann,
138 M. (2023). Microglial motility is modulated by neuronal activity and correlates with
139 dendritic spine plasticity in the hippocampus of awake mice. *eLife*, 12, e83176. <https://doi.org/10.7554/eLife.83176>
- 141 Nimmerjahn, A., Kirchhoff, F., & Helmchen, F. (2005). Resting microglial cells are highly
142 dynamic surveillants of brain parenchyma in vivo. *Science*, 308(5726), 1314–1318. <https://doi.org/10.1126/science.1110647>
- 144 Pizer, S. M., Amburn, E. P., Austin, J. D., Cromartie, R., Geselowitz, A., Greer, T., ter Haar
145 Romeny, B., Zimmerman, J. B., & Zuiderveld, K. (1987). Adaptive histogram equalization
146 and its variations. *Computer Vision, Graphics, and Image Processing*, 39(3), 355–368.
147 [https://doi.org/10.1016/S0734-189X\(87\)80186-X](https://doi.org/10.1016/S0734-189X(87)80186-X)
- 148 Prinz, M., Jung, S., & Priller, J. (2019). Microglia biology: One century of evolving concepts.
149 *Cell*, 179(2), 292–311. <https://doi.org/10.1016/j.cell.2019.08.053>
- 150 Schindelin, J., Arganda-Carreras, I., Frise, E., Kaynig, V., Longair, M., Pietzsch, T., Preibisch,
151 S., Rueden, C., Saalfeld, S., Schmid, B., & others. (2012). Fiji: An open-source platform
152 for biological-image analysis. *Nature Methods*, 9(7), 676–682. <https://doi.org/10.1038/nmeth.2019>
- 154 Tremblay, M.-È., Lowery, R. L., & Majewska, A. K. (2010). Microglial interactions with
155 synapses are modulated by visual experience. *PLOS Biology*, 8(11), 1–16. <https://doi.org/10.1371/journal.pbio.1000527>
- 157 van der Walt, S., Schönberger, J. L., Nunez-Iglesias, J., Boulogne, F., Warner, J. D., Yager,
158 N., Gouillart, E., Yu, T., & the scikit-image contributors. (2014). scikit-image: Image
159 processing in Python. *PeerJ*, 2, e453. <https://doi.org/10.7717/peerj.453>
- 160 Virtanen, P., Gommers, R., Oliphant, T. E., Haberland, M., Reddy, T., Cournapeau, D.,
161 Burovski, E., Peterson, P., Weckesser, W., Bright, J., van der Walt, S. J., Brett, M.,
162 Wilson, J., Millman, K. J., Mayorov, N., Nelson, A. R. J., Jones, E., Kern, R., Larson, E., ...
163 SciPy 1.0 Contributors. (2020). SciPy 1.0: Fundamental algorithms for scientific computing
164 in Python. *Nature Methods*, 17, 261–272. <https://doi.org/10.1038/s41592-019-0686-2>
- 165 Wall, E., Blaha, L. M., Paul, C. L., Cook, K., & Endert, A. (2018). Four perspectives on
166 human bias in visual analytics. In G. Ellis (Ed.), *Cognitive biases in visualizations* (pp.
167 29–42). Springer International Publishing. https://doi.org/10.1007/978-3-319-95831-6_3